IJE TRANSACTIONS A: Basics Vol. 33, No. 1, (January 2020) 92-104

International Journal of Engineering

Journal Homepage: www.ije.ir

Using Dynamic Thermal Rating and Energy Storage Systems Technologies Simultaneously for Optimal Integration and Utilization of Renewable Energy Sources

M. Abbasi[a], M. Sharafi Miyab[a], B. Tousi*[a], G. B. Gharehpetian[b]

[a] *Department of Electrical Engineering, Urmia University, Urmia, Iran*
[b] *Department of Electrical Engineering, Amirkabir University of Technology, Tehran, Iran*

P A P E R I N F O

Paper history:
Received 22 September 2019
Received in revised form 02 November 2019
Accepted 08 November 2019

Keywords:
Dynamic Thermal Rating
Energy Storage System
Optimization
Renewable Energy Sources
Static Thermal Rating

A B S T R A C T

Nowadays, optimal integration and utilization of renewable energy sources (RES) are of the most challenging issues in power systems. The wind and solar generation units' maximum production may or may not occur at peak consumption times resulting in non-optimal utilization of these resources. As a solution to this problem, energy storage systems (ESS) are embedded in networks. However, the power transfer from RES to ESS may lead to network congestion. In this paper, the simultaneous application of dynamic thermal rating (DTR) technology and ESS devices is proposed. The DTR is used to overcome the problem of transmission lines limited capacity and ESS is responsible for mitigating curtailment of RESs energy production by saving their generated energy in non-peak hours. The RESs generation and lines' ratings are calculated based on hourly actual weather elements. For evaluating the proposed method, a linearized formulation of DC-OPF is used in the problem definition and also simulated on a modified IEEE 30-bus test system including a wind farm, solar park, and ESS devices by using MATLAB software. In addition, different comparisons are performed demonstrating the remarkable and better performance of the proposed method compared to previously introduced methods.

***doi**: 10.5829/ije.2020.33.01a.11*

NOMENCLATURE

θ_{jk}	Voltage angles difference between j and k (non-ref. buses)	$P_{jk,\max}^{STR_l}$	Line power limit in STR state
B_{jk}	Line susceptance difference between j and k (non-ref. buses)	$P_{g,t}^{up}$	Ramp up of generating unit g in period t
$C_g^P(.)$	Active power generation cost [$/h]	$P_{g,t}^{dn}$	Ramp down of generating unit *g* in period t
$C_g^R(.)$	Reserve procurement cost [$/h]	$p_{PV,t}$	Power output of solar plant
$C_g^{su}(.)$	Generating unit start-up cost [$/h]	$P_{PV,t}^{Max}$	Maximum generation of solar plant
$C_g^{sd}(.)$	Generating unit shut-down cost [$/h]	$P_{w,t}^{Max}$	Maximum generation of wind plant
DT_g	Minimum down time of unit g	$p_{w,t}$	Power output of wind plant
G_g	Number of initial periods during which unit *j* must be online	RD_g	Ramp-down limit of unit g
L_g	Number of initial periods during which unit *g* must be offline	RU_g	Ramp-up limit of unit g
$p_{g,t}^G$	Power output of unit *g* in period t	SD_g	Shutdown ramp limit of unit g
$p_{g,\max}^G$	Maximum power output of unit *g*	SU_g	Startup ramp limit of unit *g*
$p_{g,\min}^G$	Minimum power output of unit *g*	$S_{g,0}$	Number of periods that unit *g* has been offline prior to the first period of the time span

*Corresponding Author Email: *b.tousi@urmia.ac.ir* (B.Tousi)

Please cite this article as: M. Abbasi, M. Sharafi Miyab, B. Tousi, G. B. Gharehpetian, Using Dynamic Thermal Rating and Energy Storage Systems Technologies Simultaneously for Optimal Integration and Utilization of Renewable Energy Sources, International Journal of Engineering (IJE), IJE TRANSACTIONS A: Basics Vol. 33, No. 1, (January 2020) 92-104

$p_{g,t}^{\max}$	Maximum available power output of unit g in period t	T	Number of periods of the time span
$p_{j,t}^{D}$	Active power demand at bus *j* in period t	$U_{g,t}^{G}$	Generating unit on/off binary variable
$p_{j,k}^{l}$	Line active power flow between bus *j* and *k*	UT_g	Minimum up time of unit g
$P_{jk,\max}^{DTR_l}$	Line power limit in DTR state	$U_{g,0}^{G}$	Number of periods that unit *g* has been online prior to the first period of the time span (end of period 0)

1. INTRODUCTION

Nowadays, due to the fossil fuel depletion fact and concerns of climate changes caused by greenhouse gases increment, many countries are committed to increasing the penetration of renewable energy sources (RESs) in their power systems, especially wind and solar energies [1-3]. Therefore, numerous studies and investigations have been conducted on RESs in recent years [4-6]. In general, one of the most important challenges of utilizing RESs is their production curtailments, which can cause miscoordination with load variations. This problem can be a real challenge especially in solar power plants which their maximum production happens at noon that may not be optimal in economic terms, therefore, a solution to maximize the efficient utilization of RESs is the application of energy storage system (ESS) devices. Generally, the purpose of using ESSs is to save energy in non-peak hours and inject it into the network during peak periods. In addition, it should be noted that RESs are usually built-in remote areas due to their dependence on environmental conditions like wind speed and radiation [7]. Consequently, power transfer will be needed to store their generated power, which in turn may lead to network congestion caused by the limited capacity of transmission lines. Moreover, power networks operate nowadays close to their thermal limits [8]. This transmission line limited capacity can prevent from increasing the integration of RESs in power systems. For solving this problem, building new lines or upgrading the old lines are available and practical solutions, but they are also costly and time-consuming solutions that face many barriers to environmental permits [7, 9]. The solutions based on smart grids show that there are potentials to use the existing network more effectively [10]. As indicated in [11, 12], the determined thermal rating of transmission lines is conservative compared to its actual capacity. The thermal rating of transmission lines is calculated by considering the worst weather conditions such as low wind speed and high ambient temperature and in general, a fixed value is determined for a season or a year called static thermal rating (STR) [13]. These conservative assumptions limit the carrying capacity of the lines when better weather condition prevails. The dynamic thermal rating (DTR) is one of the smart grid technologies that permits the transmission conductors to work at a higher capacity depending on the weather conditions. In DTR system, the weather elements are measured online by the sensors or estimated by forecasting methods and then, are used to update the dynamic rating of the lines. Since the actual weather condition is often better than conservative assumptions, DTR allows to use all available capacity of the lines [14].

So far, some studies have been performed on the impact of ESS devices on the integration of RESs. In [15], an approach in optimal power flow framework has been introduced to add ESS to power systems to overcome the uncertainty of wind energy. According to [15], storage devices can mitigate the variability problem of renewable sources since ESSs can provide an efficient way to utilize the network elements including generation units. In [16], a method has been presented to determine the optimal location and size of ESS in the power system with uncertain wind power modeled using a scenario of a tree. In the mentioned paper, authors have proved that by augmenting the capital investment on ESS devices, the daily operating cost of the power network can be notably reduced. However, in the abovementioned studies, the limited capacity problem of transmission lines and the impact of increasing line capacity on optimal integration and utilization of RESs have not been considered.

Furthermore, several studies have been conducted on the impact of DTR on the RESs integration in power systems. In [7], the benefits of employing DTR technology for increasing the integration of wind power in a distribution system have been presented. As indicated in [7], the optimal size of integrated wind farms in the network can be increased to 3 times when DTR is applied to the lines. Moreover, in [17], the effect of DTR on resolving the network congestion problem for increasing wind energy integration has been investigated. In this paper, authors have presented a partial least squares model based on field measurements for overhead lines dynamic rating in wind intensive areas. In [12], Kazerooni et al have presented a fairly thorough investigation of the DTR application for facilitating wind energy integration. In this paper, the best location for installing temperature monitoring facilities has been initially determined and then, a potential benefit of DTR for a power network has been discussed. According to the results presented in [12], constraint cost can be reduced by about 53% by monitoring conductors' real-time temperatures. Additionally, the advantages of DTR in the distribution

network have been presented in [17] and also its impact on the reliability of the network has been investigated in different load and DG penetration levels. According to [17], significant reliability benefits could be achieved by employing DTR technology. It has been demonstrated in [17] that these benefits are more remarkable in systems with overhead lines and also with high load levels. However, in these studies, the increment of RESs integration, especially wind energy, has been discussed without paying attention to their optimal operation. Generally, most of the researches have been focused on wind energy and solar energy has not widely been investigated.

In this paper, using DTR technology along with ESS is proposed for achieving optimal integration and utilization of RESs in power network by solving both problems of the RESs production variability and the transmission lines limited capacity. Here, transmission lines are hourly rated based on actual weather conditions. Then optimal dispatching for generating units, RESs and ESS devices are also hourly performed by solving linearized DC-OPF problems in MATLAB environment. As shown by both daily and yearly simulation results, the superiority of the proposed method over other methods is obvious due to its ability to simultaneously solve the limited capacity problem of the transmission lines and the production variability problem of the RESs resulting in higher integration and utilization of RESs in power networks.

2. PROBLEM FORMULATION

In this section, mathematical equations and related explanations are comprehensively presented for solar and wind plants, ESS devices, DTR and their incorporation in a real-time linearized DC optimal power flow (DC-OPF) problem. The optimization problem is a multi-period OPF that is time-linked through the DTR equations. In addition, the evaluation criteria are presented here.

2. 1. DTR-based Calculation of Maximum Capacity of Conductor According to IEEE Standard 738, calculation of maximum capacity of a conductor in steady-state is based on the heat balance equation as follows [18]:

$$P_j + P_s = P_c + P_r \tag{1}$$

where, P_j, $P_{s,}$ and P_c are ohmic losses heating, solar heating, cooling via convection and radiant cooling, respectively. The term of ohmic losses heat (P_j) is expressed as follows:

$$P_j = I^2 k R_{dc}[1+\alpha(\mathrm{T}_c - \mathrm{T}_a)] \tag{2}$$

where, I, R_{dc}, α, T_a, and k are conductor current, DC resistance, temperature coefficient of the conductor, ambient temperature and the skin effect coefficient, respectively. In addition, T_c represents the conductor temperature. The terms P_s, $P_{c,}$ and P_r are calculated based on IEEE Standard 738 model [18].

To calculate maximum allowable current related to the maximum allowable temperature of the conductor surface, (1) can be written as below:

$$P_j = P_c + P_r - P_s \tag{3}$$

By substituting (2) in (3), the following term is obtained:

$$I^2 k R_{dc}[1+\alpha(\mathrm{T}_c - \mathrm{T}_a)] = P_c + P_r - P_s \tag{4}$$

Consequently, by substituting the conductor temperature at the maximum allowable temperature, the maximum allowable conductor current can be obtained as given below:

$$I_{\max} = \sqrt{\frac{P_c + P_r - P_s}{k R_{dc}[1+\alpha(\mathrm{T}_c - \mathrm{T}_a)]}} \tag{5}$$

Therefore, the DTR of a transmission line can be computed by (5) when the actual weather condition is used instead of constant weather condition (STR).

2. 2. ESS Model Storage devices are characterized by their rated power (ξ), rated energy (ψ) and efficiencies (a_D and a_C) [15]. In fact, the ESS provides a time shift power flow at a specified location, considering its ability to absorb power from the network as well as injecting power to the network [19]. According to [15], the next charging status of ESS depends on its current charging status and also the charging and discharging rates as given below:

$$\delta_{t+1,j} = \delta_{t,j} + \left[\alpha_{Cj}\gamma_{t,j} - (1/\alpha_{Dj})\beta_{t,j}\right]\lambda_t \tag{6a}$$

$$0 \le \beta_{t,j} \le \psi_j \tag{6b}$$

$$0 \le \gamma_{t,j} \le \psi_j \tag{6c}$$

$$0 \le \delta_{t,j} \le \xi_j \tag{6d}$$

where, δ, β, γ, λ_t, a_C and a_D are charging status, discharging rate, charging rate, duration of the time slice, charging efficiency and discharging efficiency of ESS, respectively [15]. In addition, indexes t and j represent time and bus number, respectively.

2. 3. Wind Farm Model The wind farm is an energy conversion system whose generated energy depends on two components: kinetic energy of wind and

also wind turbines [19]. The output power of a wind farm depends on the number of wind turbines working. In this paper, the power curve of the wind turbine is utilized to model a wind farm and its output power is not considered as a constant value during the day. According to [20], the output power of the wind turbine can be expressed as a function of wind speed as follows:

$$P(\mathrm{V}_W)=\begin{cases} 0 & 0\le V_W \le V_{ci} \\ (\mathrm{A}+\mathrm{B}V_W+\mathrm{C}V_W^2)\mathrm{P}_r & V_{ci}\le V_W \le V_r \\ P_r & V_r \le V_W \le V_{co} \\ 0 & V_W \ge V_{co} \end{cases} \quad (7a)$$

where, V_W and P_r are the wind speed and rated power of the wind turbine, respectively. In addition, V_{ci}, $V_{r,}$ and V_{co} are cut-in, rated and cut-out speed of the turbine, respectively. The output power of the wind turbine is shown in Figure 1.

Finally, according to [20], coefficients A, B and C used in (7a) can be obtained as follows:

$$A=\frac{1}{(\mathrm{V}_{ci}-\mathrm{V}_r)^2}\left[\mathrm{V}_{ci}(\mathrm{V}_{ci}+\mathrm{V}_r)-4(\mathrm{V}_{ci}\mathrm{V}_r)\frac{(V_{ci}+V_r)^3}{2V_r}\right] \quad (7b)$$

$$B=\frac{1}{(\mathrm{V}_{ci}-\mathrm{V}_r)^2}\left[4(\mathrm{V}_{ci}+\mathrm{V}_r)\frac{(V_{ci}+V_r)^3}{2V_r}-(3\mathrm{V}_{ci}+\mathrm{V}_r)\right] \quad (7c)$$

$$C=\frac{1}{(\mathrm{V}_{ci}-\mathrm{V}_r)^2}\left[2-4\frac{(V_{ci}+V_r)^3}{2V_r}\right] \quad (7d)$$

2. 4. Solar Power Plant Model In the direct conversion, the photovoltaic system or PV is used to convert solar radiation into electrical energy and power plants based on this method are called solar parks that are used here. The output power of the solar park is not constant and differs based on solar radiation and environmental conditions during the day. According to [21], the output power of the PV unit is calculated for solar radiation of s as:

$$P_{PVo}(s)=N\times FF\times V_y\times I_y \quad (8a)$$

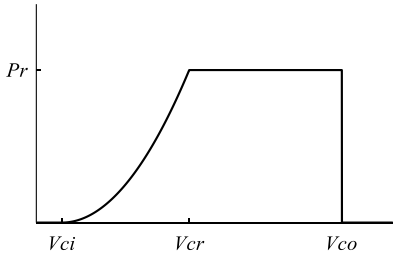

Figure 1. Wind turbine output power

where,

$$FF=\frac{V_{MPP}\times I_{MPP}}{V_{oc}\times I_{SC}} \quad (8b)$$

$$V_y=V_{oc}-K_v\times T_{cy} \quad (8c)$$

$$I_y=s[\mathrm{I}_{SC}+K_i\times(\mathrm{T}_{cy}-25)] \quad (8d)$$

$$\mathrm{T}_{cy}=T_A+s\left(\frac{N_{OT}-20}{0.8}\right) \quad (8e)$$

where N is the number of PV modules. Additionally, T_{cy} and T_A are cell temperature and ambient temperature (℃), respectively. Also, K_i and K_v are temperature coefficients of current and voltage (A/℃ and V/℃), respectively. In addition, N_{OT} is the nominal operating temperature of the cell (℃), FF is fill factor, V_{OC} and I_{SC} are open circuit voltage and short circuit current, respectively. Moreover, V_{MPP} and I_{MPP} are the voltage and current of the maximum power point.

2. 5. Optimal Power Flow The optimal Power Flow (OPF) is a well-known and challenging optimization problem which is non-convex by nature. In [22], a relaxed linearized formulation for DC load flow equations has been presented. Here, the mentioned formulations are adapted to the OPF problem. In particular, for the DC model, we assume that:

I. The susceptance is large relative to the conductance, as given in (9a)
II. The phase angle difference is small enough, as presented in (9b-9c)
III. The voltage magnitudes are close to one as given in (9d) and do not vary significantly.

$$|g|<<|b| \quad (9a)$$

$$\cos\left(\Theta_n^0-\Theta_m^0\right)\approx 1.0 \quad (9b)$$

$$\sin\left(\Theta_n^0-\Theta_m^0\right)\approx \Theta_n^0-\Theta_m^0 \quad (9c)$$

$$|\tilde{V}|\simeq 1 \quad (9d)$$

By using the above-mentioned approximations, the active power flows of the transmissions lines can be written as expressed in (9e) and reactive power flows would be equal to zero. It should be noted that this approximation is considered to be valid for ESS because ESS affects active power and its impact on reactive power is so low that could be neglected [26].

$$P_{nm}=-b_{nm}(\Theta_n^0-\Theta_m^0) \quad (9e)$$

The linearized OPF can be formulated as shown in (10) which its objective is considered as a cost function including the total production cost of active powers of generation units and their respective reserve provision costs, their start-up and shut-down costs. A Mixed-Integer Linear Thermal constraint [23] is used here for the OPF problem. The generation limits of each unit are expressed in (10b)-(10c). The maximum output power of the unit g is also constrained by ramp-up and startup ramp rates as presented in (10d), as well as by shutdown ramp rates presented in (10e). Furthermore, ramp-down limits, imposed on the power output, are given in (10f). The minimum up and down time constraints are presented in (10g)–(10l). The active power balance equations that include unit generations, wind, and solar plant productions, charging and discharging of ESSs and load demand, are expressed by (10o) and (10p). Moreover, the maximum allowable active power flow of transmission lines in STR and DTR states is given by (10q)–(10r). The generation limits of wind and solar plants are presented by (10s)-(10t). In addition, the ESS constraints are given in (10v).

$$\min \sum_{t}\sum_{g} C_g^{p}\left(P_{g,t}^{G},u_{g,t}^{G}\right)+C_g^{R}\left(P_{g,t}^{up},P_{g,t}^{dn}\right) +C_g^{su}\left(u_{g,t}^{G}\right)+C_g^{sd}\left(u_{g,t}^{G}\right) \tag{10a}$$

Subjects to:

$$P_{g,min}^{G}U_{g,t}^{G} \le P_{g,t}^{G} \le p_{g,t}^{max} \quad , \quad \forall \mathrm{g} \grave{\mathrm{o}} \mathrm{G},\ \forall \mathrm{t} \in \mathrm{T} \tag{10b}$$

$$0 \le p_{g,t}^{max} \le P_{g,max}^{G}U_{g,t}^{G} \quad , \quad \forall g \grave{o} G, \forall t \in T \tag{10c}$$

$$p_{g,t}^{max} \le P_{g,t-1}^{G} + RU_g U_{g,t-1}^{G} + SU_g\left(U_{g,t}^{G}-U_{g,t-1}^{G}\right) + P_{g,max}^{G}\left(1-U_{g,t}^{G}\right) \quad , \quad \forall g \grave{o} G, \forall t \in T \tag{10d}$$

$$p_{g,t}^{max} \le P_{g,max}^{G}U_{g,t+1}^{G} + SD_g\left(U_{g,t}^{G}-U_{g,t+1}^{G}\right) \quad , \quad \forall g \grave{o} G, \forall t = 1\ldots T-1 \tag{10e}$$

$$P_{g,t-1}^{G} - P_{g,t}^{G} \le RD_g U_{g,t}^{G} + SD_g\left(U_{g,t-1}^{G}-U_{g,t}^{G}\right) + P_{g,max}^{G}\left(1-U_{g,t-1}^{G}\right) \quad , \quad \forall g \grave{o} G, \forall t \in K \tag{10f}$$

$$\sum_{t=1}^{G_g}\left(1-U_{g,t}^{G}\right) = 0 \ , \ \forall g \grave{o} G \tag{10g}$$

$$\sum_{n=t}^{t+UT_g-1} U_{g,n}^{G} \ge UT_g\left(U_{g,t}^{G}-U_{g,t-1}^{G}\right) \quad , \forall g \grave{o} G \ , \forall t = G_g+1\ldots T-UT_g+1 \tag{10h}$$

$$\sum_{n=t}^{T}\left[U_{g,n}^{G}-\left(U_{g,t}^{G}-U_{g,t-1}^{G}\right)\right] \ge 0 \quad , \forall g \grave{o} G \ , \forall t = T-UT_g+2\ldots T \tag{10i}$$

$$\sum_{t=1}^{L_g} U_{g,t}^{G} = 0 \ , \ \forall g \grave{o} G \tag{10j}$$

$$\sum_{n=t}^{t+DT_g-1}(1-U_{g,n}^{G}) \ge DT_g\left(U_{g,t-1}^{G}-U_{g,t}^{G}\right) \quad , \forall g \grave{o} G \ , \forall t = L_g+1\ldots T-DT_g+1 \tag{10k}$$

$$\sum_{n=t}^{T}\left[1-U_{g,n}^{G}-\left(U_{g,t-1}^{G}-U_{g,t}^{G}\right)\right] \ge 0 \quad , \forall g \grave{o} G \ , \forall t = T-DT_g+2\ldots T \tag{10l}$$

$$G_g = \min\left[T,(\mathrm{UT}_g-\mathrm{U}_{g,0})\,\mathrm{U}_{g,0}^{G}\right] \tag{10m}$$

$$L_g = \min\left[T,(D\,\mathrm{T}_g-S_{g,0})(1-\mathrm{U}_{g,0}^{G})\right] \tag{10n}$$

$$\sum_{\Omega_g - j} P_{g,t}^{G} + p_{PV,t} + p_{w,t} - P_{\mathrm{j,t}}^{D} + \left(\beta_{j,t}-\gamma_{j,t}\right) + P_{g,t}^{up} - P_{g,t}^{dn} = \sum_{k}^{j\neq k} P_{\mathrm{jk,t}}^{l} \tag{10o}$$

$$P_{\mathrm{jk,t}}^{l} = B_{jk,t}\theta_{jk,t} \tag{10p}$$

$$-P_{jk,\max}^{STR_l} \le P_{jk,t}^{l} \le P_{jk,\max}^{STR_l} \tag{10q}$$

$$-P_{jk,\max}^{DTR_l} \le P_{jk,t}^{l} \le P_{jk,\max}^{DTR_l} \tag{10r}$$

$$p_{PV,t} \le P_{PV,t}^{Max} \tag{10s}$$

$$p_{w,t} \le P_{w,t}^{Max} \tag{10t}$$

$$U_{g,t}^{G} = \begin{cases} 1 & \text{if unit } g \text{ is on} \\ 0 & \text{if unit } g \text{ is off} \end{cases} \tag{10u}$$

and (6a)-(6d) (10v)

It should be noted that the formulated optimization problems are Mixed-Integer Quadratically Constrained (MIQCP) and Quadratically Constrained optimization (QCP) programs. These types of optimization problems can be easily solved using conventional software. In our case, they are solved using the Mosek package [24] via the MATLAB interface YALMIP [25].

TABLE 1. Generator data

	Bus No.	P_G^{min} *[MW]*	P_G^{max} *[MW]*	Cost coefficients			
				a [$/MW^2]	b[$/MW]	c [$]	*Ramp up/down* [$/MW]
G1	1	50	200	0.00375	2	0	0.2
G2	2	20	80	0.0175	1.75	0	0.175
G13	22	15	50	0.0625	1	0	0.1
G22	27	10	35	0.00834	3.25	0	0.325
G23	23	10	30	0.025	3	0	0.3
G27	13	12	40	0.025	3	0	0.3

2. 6. Evaluation Criteria By considering the increase of RESs integration and reduction of network costs as the main contribution of this paper, the evaluation criteria can be introduced as expressed below:

- Amount of annual curtailed energy for the wind farm and solar park.
- Annual cost of generation.

For the first criteria, two indexes are defined as curtailed wind power (*CWP*) and curtailed solar power (*CSP*) which are expressed by the following equations:

$$CWP = \sum_{h=1}^{8760} WP_h \,(\text{MWh/ yr}) \tag{11}$$

$$CSP = \sum_{h=1}^{8760} PVP_h \,(\text{MWh/ yr}) \tag{12}$$

where, WP_h, and PVP_h are the curtailments of wind and solar powers at the hour h, respectively. The second criterion describes the annual operational costs of generating units that can be calculated from the objective function for a period of one year.

3. CASE STUDY

Figure 2 shows the single-line diagram of the modified IEEE 30-bus system [26] which includes 30 buses, 41 lines and 6 generating units. Also, a wind farm with a maximum power of 70 MW and a solar park with a maximum power of 60 MW are embedded in the network at the buses 17 and 30, respectively. The reason that solar unit is considered to be installed at an end bus is because of this fact that solar power plants are usually built-in remote areas with high radiation. In addition, two ESS devices are placed on buses No. 4 and 21. The maximum capacity of ESS devices is 300 MWh and their maximum power rate is considered to be 30 MW. As seen in Figure 2, we have divided this network into three areas named 1, 2 and 3. Also, it is assumed that regions are close to each other. In addition, different weather data are used for each area. The data used in this paper is the weather data of Tabriz city of Iran, that is available in literature [1].

According to [27], the wind speed can be suitably described using the time-series auto-regressive and moving-average (ARMA) model and the actual wind speed trend can be simulated. For area 1, the actual data of the wind speed is used and for the others, the ARMA model is fitted. To fit the ARMA model for areas 2 and 3, the actual wind speed data of area 1 is used as original data. For ambient temperature, the actual temperature data is used for area 1. Also, the temperature data for areas 2 and 3 are considered to be 4 degrees warmer and 5 degrees colder than area 1. The

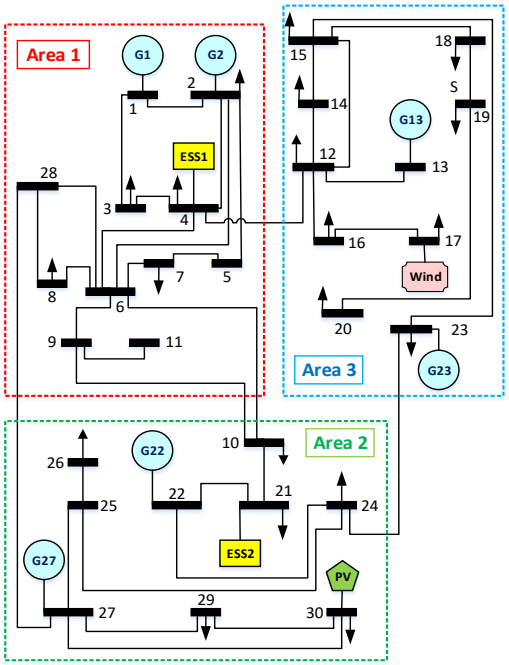

Figure 2. Single-line diagram of the modified 30-bus system

[1] https://pvwatts.nrel.gov/

information of the IEEE 30-bus system including generators data and active load data are given in Table 1 and Table 2, respectively. In addition, lines reactance (X) data are presented in Table 3.

Due to this fact that the implementation of DTR equipment on all of the transmission lines is not economic, so far, various methods have been introduced for selecting an optimal number of candidate lines. For achieving this aim, the presented method in [28] is employed in this paper. By using this method, 11 lines out of 41 lines of the test system are selected to have DTR as listed in Table 3.

TABLE 2. Load data for 30-bus test system

Bus No.	Active power (MW)	Bus No.	Active power (MW)
1	0	16	3.5
2	21.7	17	9
3	2.4	18	3.2
4	7.6	19	9.5
5	94.2	20	2.2
6	0	21	17.5
7	22.8	22	0
8	30	23	3.2
9	0	24	8.7
10	5.8	25	0
11	0	26	3.5
12	11.2	27	0
13	0	28	0
14	6.2	29	2.4
15	8.2	30	10.6

TABLE 3. Line data for 30-bus system along with DTR data

From	To	X	DTR	From	To	X	DTR
1	2	0.06 j	No	15	18	0.22 j	**Yes**
1	3	0.19 j	No	18	19	0.13 j	No
2	4	0.17 j	No	19	20	0.07 j	No
3	4	0.04 j	No	10	20	0.21 j	No
2	5	0.20 j	No	10	17	0.08 j	**Yes**
2	6	0.18 j	No	10	21	0.07 j	No
4	6	0.04 j	No	10	22	0.15 j	No
5	7	0.12 j	No	21	22	0.02 j	No
6	7	0.08 j	No	15	23	0.20 j	**Yes**
6	8	0.04 j	No	22	24	0.18 j	**Yes**
6	9	0.21 j	No	23	24	0.27 j	**Yes**
6	10	0.56 j	No	24	25	0.33 j	No
9	11	0.21 j	No	25	26	0.38 j	No
9	10	0.11 j	No	25	27	0.21 j	**Yes**
4	12	0.26 j	No	28	27	0.40 j	No
12	13	0.14 j	No	27	29	0.42 j	**Yes**
12	14	0.26 j	No	27	30	0.60 j	**Yes**
12	15	0.13 j	No	29	30	0.45 j	**Yes**
12	16	0.20 j	No	8	28	0.20 j	No
14	15	0.20 j	No	6	28	0.06 j	**Yes**
16	17	0.19 j	**Yes**				

4. SIMULATION RESULTS

All simulations have been performed by MATLAB software using YALMIP toolbox [28]. Four different scenarios have been considered as follow:

Scenario 1 (STR): lines are rated by STR and there is no ESS in power network (base case).

Scenario 2 (STR+ESS): lines are rated by STR and power system includes ESS devices

Scenario 3 (DTR): lines are rated by DTR and there is no ESS in system

Scenario 4 (DTR+ESS): lines are rated by DTR and power system includes ESS devices

Simulations have been carried out for all scenarios for a one-year period and the results have been evaluated. Also, for more investigations, daily simulations have been performed for each scenario and the results have been discussed, as well.

4. 1. Annual Results

4. 1. 1. Results for 1pu Load Level After the determination of weather parameters, the system is simulated with daily planning for a period of one year based on the hourly dispatch. It should be noted that the generation of renewable energy sources is not constant, so it should be calculated per hour for both solar parks and wind farms in a whole year. In addition, selected transmission lines are hourly rated based on the weather parameters of their location. Simulations are performed for all scenarios and annual costs as well as CWP and CSP indices are compared in Table 4. As seen, the highest operational cost and energy curtailment belong to the STR case. It is clearly due to limited line capacity and network defect in overcoming the intermittent generation of RES.

The results for scenario 2 (STR+ESS), listed in Table 4, indicate that using ESS devices in the network without any improvement on the lines' capacity is more effective on the reduction of operational costs than the energy curtailment of RESs. Because the efficient

charging and discharging of ESS devices results in a smoother load profile for generating units leading to reduced ramp up/down costs of generating units. Also, ESS devices by storing RES energies at off-peak periods and delivering it to the network at peak periods, help the system to reduce the operational costs. But due to the lack of influence on the capacity of lines, ESSs cannot completely prevent the energy curtailment of RESs.

Moreover, based on the results of scenario 3, using DTR technology in addition to optimizing the power plant generation by solving the problem of limited lines capacity, increases the penetration of RES in the network significantly. But it is not fully satisfactory, because it is better for free energies to be stored at off-peak hours and injected into the network at peak hours. By comparing the results of scenario 4 (DTR+ESS) with others in Table 4, it is evident that both operational cost and amount of curtailed energy are significantly reduced in the last scenario. The DTR releases the latent capacity of transmission lines and provides suitable conditions for integrating RESs into a network or transferring their energy to ESS devices. In other words, ESS prevents from the curtailment of more energy by storing it. The ESS devices optimize the operation of RESs by absorbing their energies at off-peak hours and delivering it to the network at peak hours. So, these two technologies (DTR and ESS) perfectly complement each other.

4. 1. 2. Results for 0.75pu and 1.2pu Load Level

The results are listed in Table 5 and Table 6 for the period of one year. Other data needed for simulations are the same as the ones used for the 1pu load level, and only the network loads have been changed.

Based on the results of Table 5, it can be said that if the system load is low, ESS will have better performance compared to DTR. It is because of this fact that under low load conditions, the network should be supplied from thermal power plants due to the minimum production limit of generating units, resulting in inevitable curtailment of RES generated energy. Therefore, we definitely need to store RES generations.

By comparing the results listed in Table 6 with the results of Table 5 and Table 4, it is observed that the DTR role is more explicit in networks with a high level of load. Because in these networks, congestion and line capacity problems are more important. But it is also seen that simultaneous use of ESS and DTR leads to better results compared to others. Because the optimization program, aimed for minimizing the overall costs, tries to use RESs efficiently and because of low load during daylight hours, the RESs powers cannot be injected to the network, therefore, the perfect solution is to store the produced power and inject it into the network at peak hours. But the limited line capacity can prevent more transfer of this power to ESS devices. So, DTR, as an efficient way, helps to increase the penetration of RESs in the network by solving the problem of the network capacity.

TABLE 4. Results for the scenarios for 1pu load level

Scenario	Annual Costs ($)	CWP (MWh/yr)	CSP MWh/yr)
STR	2.8802×10^6	2.987×10^4	5.782×10^3
STR+ESS	2.8002×10^6	2.983×10^4	5.4×10^3
DTR	2.7432×10^6	4.05×10^3	2.987×10^3
DTR+ESS	2.56×10^6	3.71×10^3	1.87×10^3

TABLE 5. Results comparison for different scenarios for 0.75pu load level

Scenario	Annual costs ($)	CWP (MWh/yr)	CSP (MWh/yr)
STR	2.18×10^6	5.7226×10^4	1.1591×10^4
STR+ESS	2.097×10^6	4.3569×10^4	5.3956×10^3
DTR	2.1732×10^6	4.85×10^4	1.657×10^4
DTR+ESS	2.016×10^6	1.433×10^4	4.0217×10^3

TABLE 6. Results comparison for different scenarios for 1.2pu load level

Scenario	Annual costs($)	CWP (MWh/yr)	CSP (MWh/yr)
STR	3.916×10^6	5.392×10^4	4.0011×10^3
STR+ESS	3.8727×10^6	3.397×10^4	3.426×10^3
DTR	3.8332×10^6	8.919×10^3	901.34
DTR+ESS	3.67×10^6	7.432×10^3	0

4. 2. Daily Results

For further investigation on the impact of the proposed combination, a specific day is studied and the results are analyzed. The selected day is chosen so that the power generation of RESs is high. Weather parameters for the STR case are listed in Table 7.

Since the selected day is in the spring, the temperature of the STR case is considered equal to the maximum temperature of that season. Also, the daily active load profile and the weather parameters profile are shown in Figures 3 and 4, respectively. The powers generated by the wind farm and the solar park respectively are 1208.8 MWh and 323.6244 MWh during this day.

To compare the results of all 4 scenarios, the output power of generating units and also wind and solar energies delivered to the system, are shown in Figures 5 to 16.

Also, the objective function value for different scenarios is compared in Table 8. In addition, the delivered wind energy (DWE) and delivered solar energy (DSE) for all scenarios are listed in Table 9.

TABLE 7. Weather parameters for STR case

Wind Speed (m/s)	Ambient Temp. (°C)	Radiation (w/m^2)
0.5	15	900

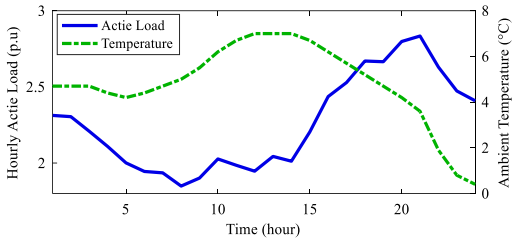

Figure 3. Daily active load in per unit (Base value 100 MW) and ambient temperature profiles.

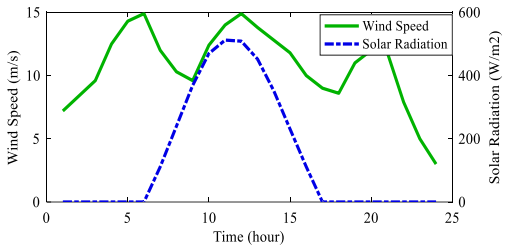

Figure 4. Daily wind speed and solar radiation profiles

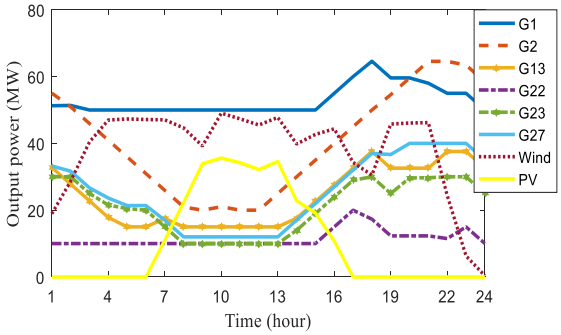

Figure 5. Output powers of all generation units for scenario 1

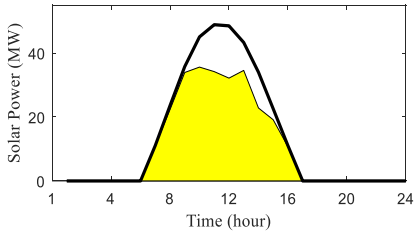

Figure 6. Injected solar power to the system for scenario 1

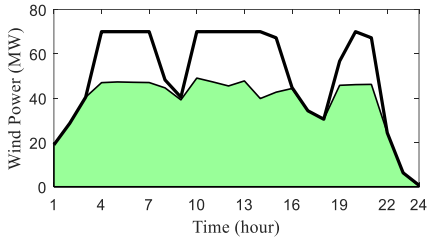

Figure 7. Injected wind power to network for scenario 1

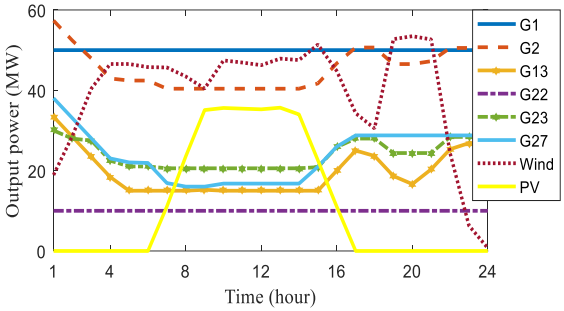

Figure 8. Output powers of all generation units for scenario 2

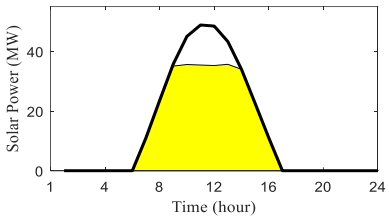

Figure 9. Injected solar power to system for scenario 2

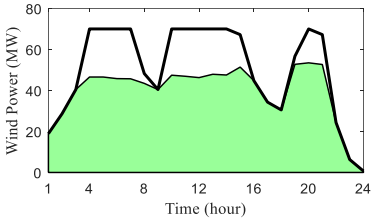

Figure 10. Injected wind power to network for scenario 2

TABLE 8. Objective function value for different scenarios

Scenario	STR	STR+ESS	DTR	DTR+ESS
Objective function value [$]	12449	11880	12026	10919

TABLE 9. Delivered wind and solar energies for scenarios

Scenario	STR	STR+ESS	DTR	DTR+ESS
DSE [MWh]	256.4291	279.2180	213.938	323.6244
DWE [MWh]	910.8499	943.6789	1087.9	1208.8
Total [MWh]	1167.279	1222.8969	1301.838	1532.4244

Figure 5 shows the output power of all generation units for scenario 1. As seen in Figure 6 and Figure 7, while none of the technologies of ESS and DTR are used, the amount of the curtailed solar and wind energies are high which is not economically and environmentally justifiable. Also, the objective function value of this scenario is 12449 $ (in Table 8) which is the highest value among the scenarios.

When only ESS devices are used in power system and lines are traditionally rated by STR (i.e. scenario 2), as it is obviously seen in Figure 8, the ESSs provide smoother load conditions for power plants and this reduces ramp up/down cost of the generating units. Also, by comparing delivered solar and wind energy for this scenario (STR+ESS), shown in Figure 9 and Figure 10, the ESS has evidently better performance in the case of solar energy rather than wind energy. Because the maximum generation of the solar park is in off-peak hours and the transmission lines have some free capacity for transferring power from solar parks to ESSs. But in the case of a wind farm, the maximum generation can occur at any time of day and it may occur in peak hours when the capacity of the most lines is in use.

As mentioned, scenario 3 just focuses on lines capacity improvement to increase RESs penetration using DTR technology. The output powers of generating units for scenario 3 are presented in Figure 11 demonstrating that ramp up/down of generating units cannot be mitigated by DTR. As seen in Figure 12 and Figure 13, the wind energy integrated into power system has increased but solar energy integration has reduced compared to the previous scenarios; It is due to this fact that the maximum solar energy generation is in accordance with minimum system load, and constraints related to minimum production of generating unit prevent from injection of more solar energy to the network and the operator should feed loads from thermal power plants. The objective function value of scenario 3 is 12026 $ (see Table 8) which means 3.4% reduction in costs compared to scenario1 but its value is higher than scenario 2 because the DTR cannot have a significant effect on optimized utilization of RESs.

Scenario 4 uses both DTR and ESS technologies in the power system. The results for unit commitment, the output power of generating units and RES production are shown in Figure 14 to Figure 16. As presented in Table 8, the objective function value of this scenario(ESS+DTR) is 10919$ which shows a reduction of about 12.3, 7.7, and 9.9% compared to scenarios 1, 2 and 3, respectively.

It is obvious that there is no RES energy curtailment in the simultaneous application of DTR and ESS. In fact, these two technologies operate are the complement of each other. The DTR solves the lines capacity limit problem and increases the penetration of RESs in the

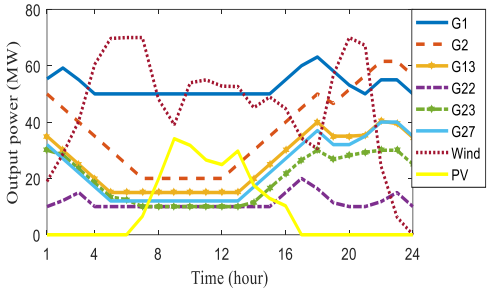

Figure 11. Output powers of all generation units for scenario 3

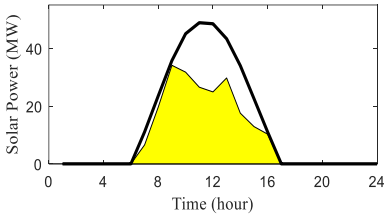

Figure 12. Injected solar power to grid for scenario 3

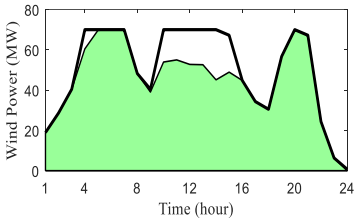

Figure 13. Injected wind power to grid for scenario 3

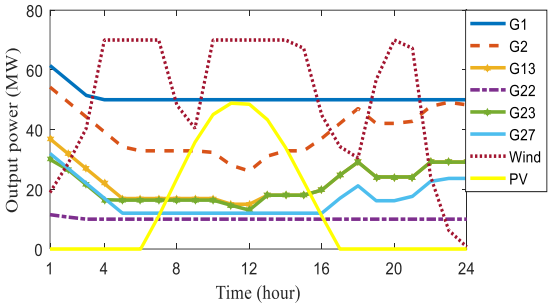

Figure 14. Output powers of all generation units for scenario 4

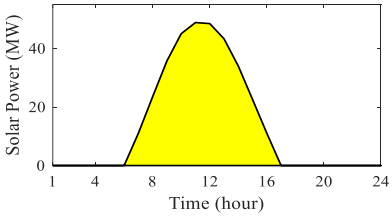

Figure 15. Injected solar power to grid for scenario 4

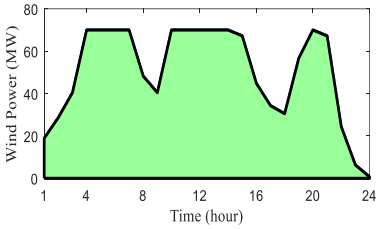

Figure 16. Injected wind power to grid for scenario 4

power system and the ESS helps the optimal utilization of RESs to reduce operational costs. Also, DTR helps to transmit more energy from RES to ESS devices by increasing lines capacity.

In addition, by comparing the state of charge of ESS 2 for scenario 2 and scenario 4 (shown in Figure 17 and Figure 18, respectively) it is obvious that the stored energy of the ESS 2 has increased by 50MWh by using the proposed combination.

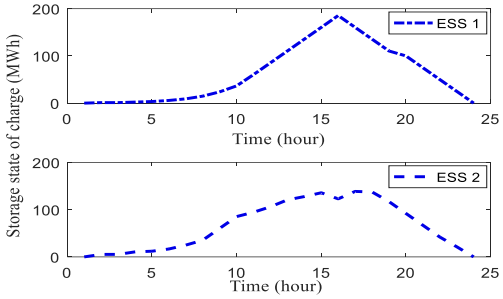

Figure 17. State of charge of ESSs for scenario 2

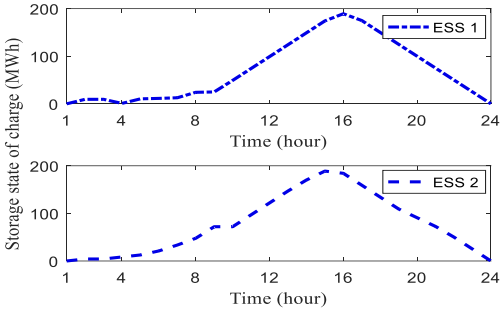

Figure 18. State of charge of ESSs for scenario 4

5. CONCLUSION

In this paper, the application of ESS devices along with DTR technology has been proposed to achieve maximum and optimal utilization of RES energies. The proposed combination has been compared with different solutions in four scenarios. The results show that the use of DTR technology increases the penetration level of RESs compared to STR technology, but due to the variable nature of RESs, the DTR technology cannot be an optimal solution. Therefore, the application of ESS devices along with DTR technology has been proposed. In addition, RESs such as wind and solar sources, are usually installed in remote areas and transferring their power to ESS devices can face the capacity limit of transmission lines which can be solved by applying DTR on transmission lines. Thus, DTR and ESS have been used as the complement of each other in this paper. The results show that the proposed combination reduces annual costs by about 11% compared to the case which has none of the mentioned technologies. Also, it reduces annual costs by about 9% and 7% compared to the cases that use only the ESS and only DTR technology, respectively. In addition, for all load levels, the proposed combination has better results than other cases. Also, daily simulations have been performed and the results show that the combination of DTR and ESS reduces operational costs by 12.3% compared to the base system. The operational costs of the proposed solution also are 9.9% and 7.7% less than the cases that just use one of them.

6. REFERENCES

1. Xu, B., Ulbig, A. and Andersson, G., "Impacts of dynamic line rating on power dispatch performance and grid integration of renewable energy sources", in IEEE PES ISGT Europe 2013, IEEE., (2013), 1-5.
2. Gholami, M., "Islanding detection method of distributed generation based on wavenet", ***International Journal of Engineering***, Vol. 32, No. 2, (2019), 242-248.
3. BARFOROSHI, T. and Adabi, J., "Distributed generation expansion planning considering load growth uncertainty: A novel multi-period stochastic model", ***International Journal of Engineering***, Vol. 31, No. 3, (2018), 405-414.
4. Nikkhah, S., Jalilpoor, K., Kianmehr, E. and Gharehpetian, G.B., "Optimal wind turbine allocation and network reconfiguration for enhancing resiliency of system after major faults caused by natural disaster considering uncertainty", ***IET Renewable Power Generation***, Vol. 12, No. 12, (2018), 1413-1423.
5. Movahedi, A., Niasar, A.H. and Gharehpetian, G., "Designing sssc, tcsc, and statcom controllers using avurpso, gsa, and ga for transient stability improvement of a multi-machine power system with pv and wind farms", ***International Journal of Electrical Power & Energy Systems***, Vol. 106, (2019), 455-466.
6. Tavakkoli-Moghaddam, R. and Mousavi, M., "Group decision making based on a new evaluation method and hesitant fuzzy setting with an application to an energy planning problem", ***International Journal of Engineering-Transactions C: Aspects***, Vol. 28, No. 9, (2015), 1303-1311.
7. Heckenbergerová, J. and Hošek, J., "Dynamic thermal rating of power transmission lines related to wind energy integration", in 2012 11th International Conference on Environment and Electrical Engineering, IEEE., (2012), 798-801.

8. Carreras, B.A., Newman, D.E., Dobson, I. and Poole, A.B., "Evidence for self-organized criticality in a time series of electric power system blackouts", ***IEEE Transactions on Circuits and Systems I: Regular Papers***, Vol. 51, No. 9, (2004), 1733-1740.
9. Roberts, D., Taylor, P. and Michiorri, A., "Dynamic thermal rating for increasing network capacity and delaying network reinforcements", ***CIRED Seminar: SmartGrids for Distribution***, (2008), 1-4.
10. Gungor, V.C., Sahin, D., Kocak, T., Ergut, S., Buccella, C., Cecati, C. and Hancke, G.P., "Smart grid technologies: Communication technologies and standards", ***IEEE Transactions on Industrial Informatics***, Vol. 7, No. 4, (2011), 529-539.
11. Abdelkader, S.M., John Morrow, D., Fu, J. and Abbot, S., "Partial least squares model for dynamic rating of overhead lines in wind intensive areas based on field measurements", ***Journal of Renewable and Sustainable Energy***, Vol. 5, No. 6, (2013), 063105.
12. Kazerooni, A., Mutale, J., Perry, M., Venkatesan, S. and Morrice, D., "Dynamic thermal rating application to facilitate wind energy integration", in 2011 IEEE Trondheim PowerTech, IEEE., (2011), 1-7.
13. Nick, M., Alizadeh-Mousavi, O., Cherkaoui, R. and Paolone, M., "Security constrained unit commitment with dynamic thermal line rating", ***IEEE Transactions on Power Systems***, Vol. 31, No. 3, (2015), 2014-2025.
14. Cigré, T., "353: Guidelines for increased utilization of existing overhead transmission lines", ***Working Group B***, Vol. 2, No., (2008), 13.
15. Oh, H., "Optimal planning to include storage devices in power systems", ***IEEE Transactions on Power Systems***, Vol. 26, No. 3, (2010), 1118-1128.
16. Xiong, P. and Singh, C., "Optimal planning of storage in power systems integrated with wind power generation", ***IEEE Transactions on Sustainable Energy***, Vol. 7, No. 1, (2015), 232-240.
17. Safdarian, A., Degefa, M.Z., Fotuhi-Firuzabad, M. and Lehtonen, M., "Benefits of real-time monitoring to distribution systems: Dynamic thermal rating", ***IEEE Transactions on Smart Grid***, Vol. 6, No. 4, (2015), 2023-2031.
18. "738-2012 - ieee standard for calculating the current-temperature relationship of bare overhead conductors", in ISBN: 978-0-7381-8887-4., (2013).
19. Gao, Y. and Billinton, R., "Adequacy assessment of generating systems containing wind power considering wind speed correlation", ***IET Renewable Power Generation***, Vol. 3, No. 2, (2009), 217-226.
20. Giorsetto, P. and Utsurogi, K.F., "Development of a new procedure for reliability modeling of wind turbine generators", ***IEEE Transactions on Power Apparatus and Systems***, Vol., No. 1, (1983), 134-143.
21. Hung, D.Q., Mithulananthan, N. and Lee, K.Y., "Determining pv penetration for distribution systems with time-varying load models", ***IEEE Transactions on Power Systems***, Vol. 29, No. 6, (2014), 3048-3057.
22. Coffrin, C. and Van Hentenryck, P., "A linear-programming approximation of ac power flows", ***Informs Journal on Computing***, Vol. 26, No. 4, (2014), 718-734.
23. Carrión, M. and Arroyo, J.M., "A computationally efficient mixed-integer linear formulation for the thermal unit commitment problem", ***IEEE Transactions on Power Systems***, Vol. 21, No. 3, (2006), 1371-1378.
24. ApS, M., "Mosek optimization toolbox for matlab", User's Guide and Reference Manual, Version, Vol. 4, (2001).
25. Löfberg, J., "Yalmip: A toolbox for modeling and optimization in matlab", in Proceedings of the CACSD Conference, Taipei, Taiwan. Vol. 3, (2004).
26. Zimmerman, R.D., Murillo-Sánchez, C.E. and Gan, D., "Matpower: A matlab power system simulation package", Manual, Power Systems Engineering Research Center, Ithaca NY, Vol. 1, (1997).
27. Teh, J. and Cotton, I., "Reliability impact of dynamic thermal rating system in wind power integrated network", ***IEEE Transactions on Reliability***, Vol. 65, No. 2, (2016), 1081-1089.
28. Chu, R., "On selecting transmission lines for dynamic thermal line rating system implementation", ***IEEE Transactions on Power Systems***, Vol. 7, No. 2, (1992), 612-619.

Using Dynamic Thermal Rating and Energy Storage Systems Technologies Simultaneously for Optimal Integration and Utilization of Renewable Energy Sources

M. Abbasi[a], M. Sharafi Miyab[a], B. Tousi[a], G. B. Gharehpetian[b]

[a] *Department of Electrical Engineering, Urmia University, Urmia, Iran*
[b] *Department of Electrical Engineering, Amirkabir University of Technology, Tehran, Iran*

P A P E R I N F O

Paper history:
Received 22 September 2019
Received in revised form 02 November 2019
Accepted 08 November 2019

Keywords:
Dynamic Thermal Rating
Energy Storage System
Optimization
Renewable Energy Sources
Static Thermal Rating

چکیده

امروزه، استفاده و ادغام بهینه سیستم های انرژی تجدیدپذیر (RES) در شبکه های قدرت از جمله موضوعات بسیار مهم و چالش برانگیز می باشند. بطورکلی، تولید ماکزیمم واحد های نیروگاهی خورشیدی و بادی می تواند در ساعات اوج مصرف اتفاق نیفتد که باعث استفاده غیر بهینه از این منابع خواهد شد. بعنوان یک راه حل برای این مشکل، سیستم های ذخیره ساز انرژی (ESS) در سیستم قدرت مورد استفاده قرار می گیرند. اما انتقال توان از RES ها به ESS ها ممکن است منجر به تراکم خطوط گردد. در این مقاله، استفاده همزمان از فناوری ریتینگ دینامیکی گرمایی (DTR) خطوط و تجهیزات ESS برای رفع مشکلات بالا پیشنهاد می شود. DTR برای فائق آمدن بر مشکل محدودیت خطوط انتقال مورد استفاده قرار می گیرد و ESS مسوولیت کاهش قطع تولید انرژی RES ها را با ذخیره سازی انرژی تولیدی این نیروگاه ها در زمان های مصرف غیرپیک، بر عهده می گیرد. تولیدات RES ها و ریتینگ خطوط بر اساس عناصر آب و هوایی واقعی بر حسب ساعت محاسبه می گردند. برای ارزیابی روش پیشنهادی، از یک فرمولبندی خطی شده از DC-OPF استفاده می شود و همچنین روش پیشنهادی بر روی سیستم اصلاحی IEEE ۳۰ باسه استاندارد شامل مزرعه بادی، پارک خورشیدی و دستگاه های ذخیره ساز انرژی، با استفاده از نرم افزار متلب شبیه سازی می شود. بعلاوه، مقایسات مختلفی انجام می گیرد که نشانگر عملکرد بهتر و قابل توجه روش پیشنهادی نسبت به روش های قبلی می باشد.

***doi**: 10.5829/ije.2020.33.01a.11*